

Supporting Information

Electrochemical Construction of Hierarchically Ordered CdSe Sensitized TiO₂ Nanotube Arrays: Towards Versatile Photoelectrochemical Water Splitting and Photoredox Applications

*Fang-Xing Xiao, Jianwei Miao, Hsin-Yi Wang, Hongbin Yang, Jiazang Chen, Bin Liu**

School of Chemical and Biomedical Engineering, Nanyang Technological University, 62
Nanyang Drive, Singapore 637459, Singapore. Fax: (65) 6794-7553; Tel: (65) 6513-7971; E-
mail:liubin@ntu.edu.sg

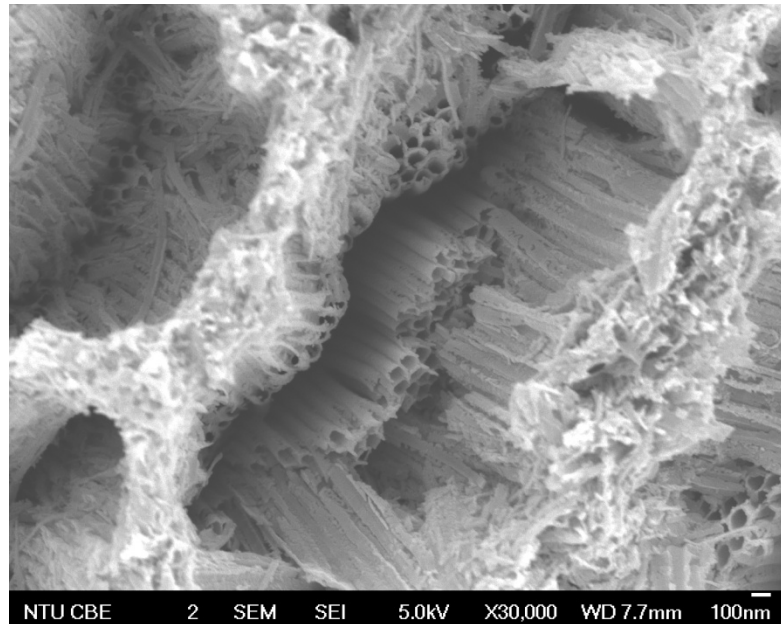


Figure S1. FESEM image of TiO₂ nanotube arrays prepared by conventional one-step anodization strategy.

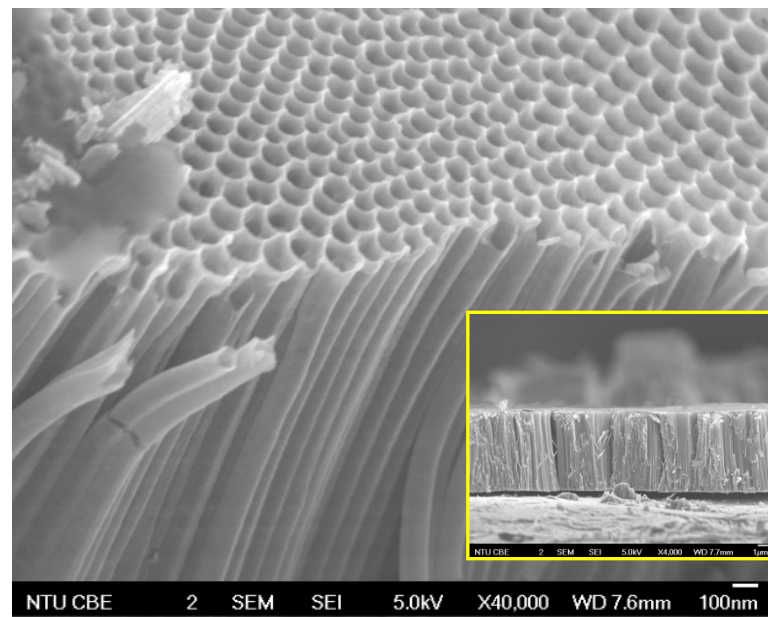


Figure S2. Cross-sectional FESEM image of NP-TNTAs prepared by two-step anodization approach.

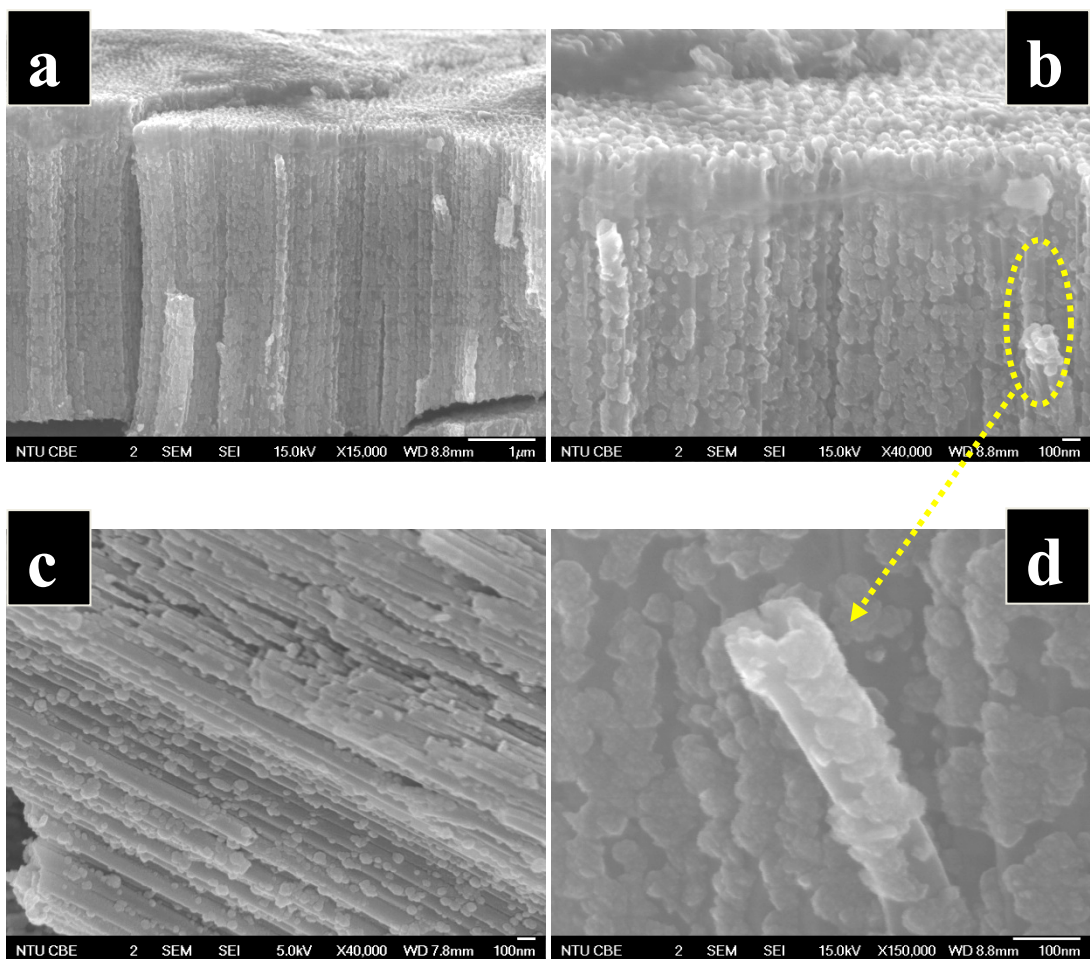


Figure S3. Cross-sectional images of CdSe/NP-TNTAs heterostructure (1600 s).

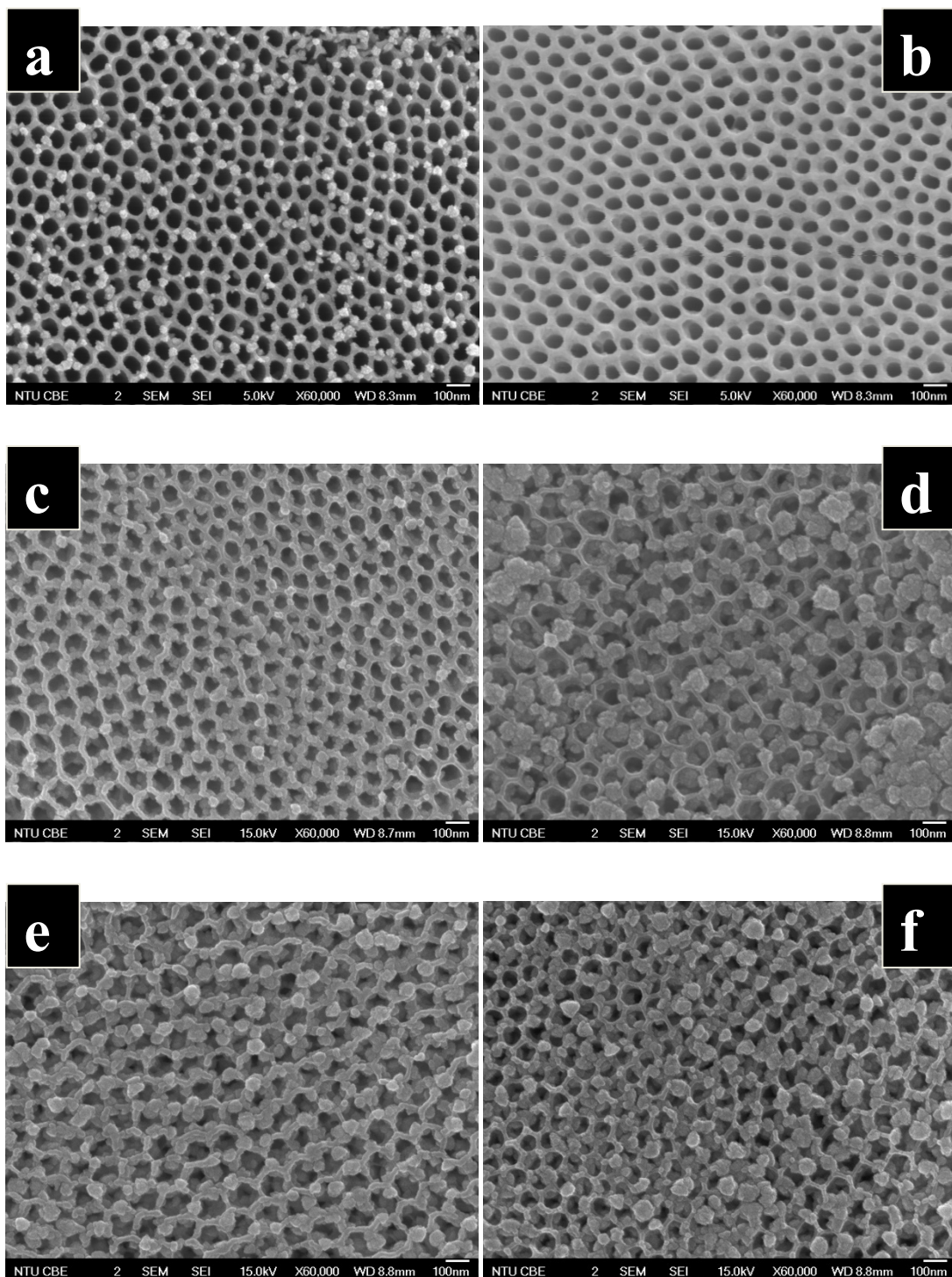


Figure S4. FESEM images of CdSe/NP-TNTAs heterostructures prepared *via* electrochemical deposition approach with different deposition time, (a) 400 s, (b) 800 s, (c) 1000 s, (d) 1200 s, (e) 1800 s, and (f) 2000 s.

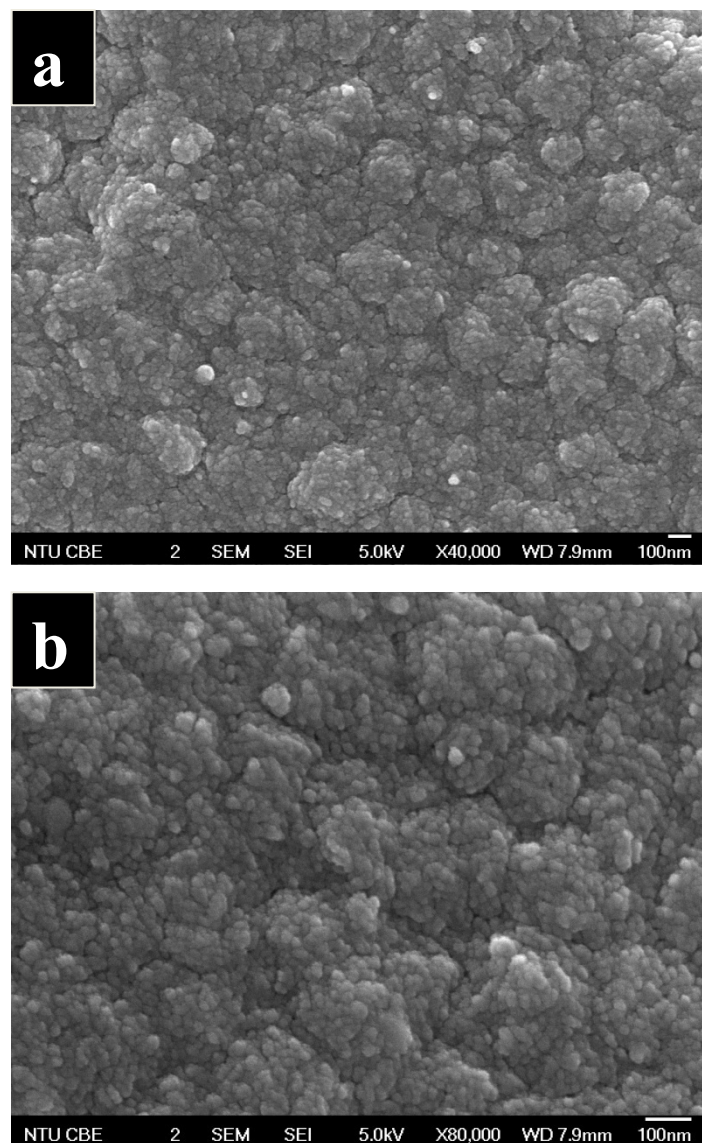


Figure S5. (a) Low-magnified and (b) high-magnified FESEM images of pure CdSe film (1600 s) deposited on Ti foil under otherwise the same experimental conditions, apart from replacing NP-TNTAs substrate with Ti foil.

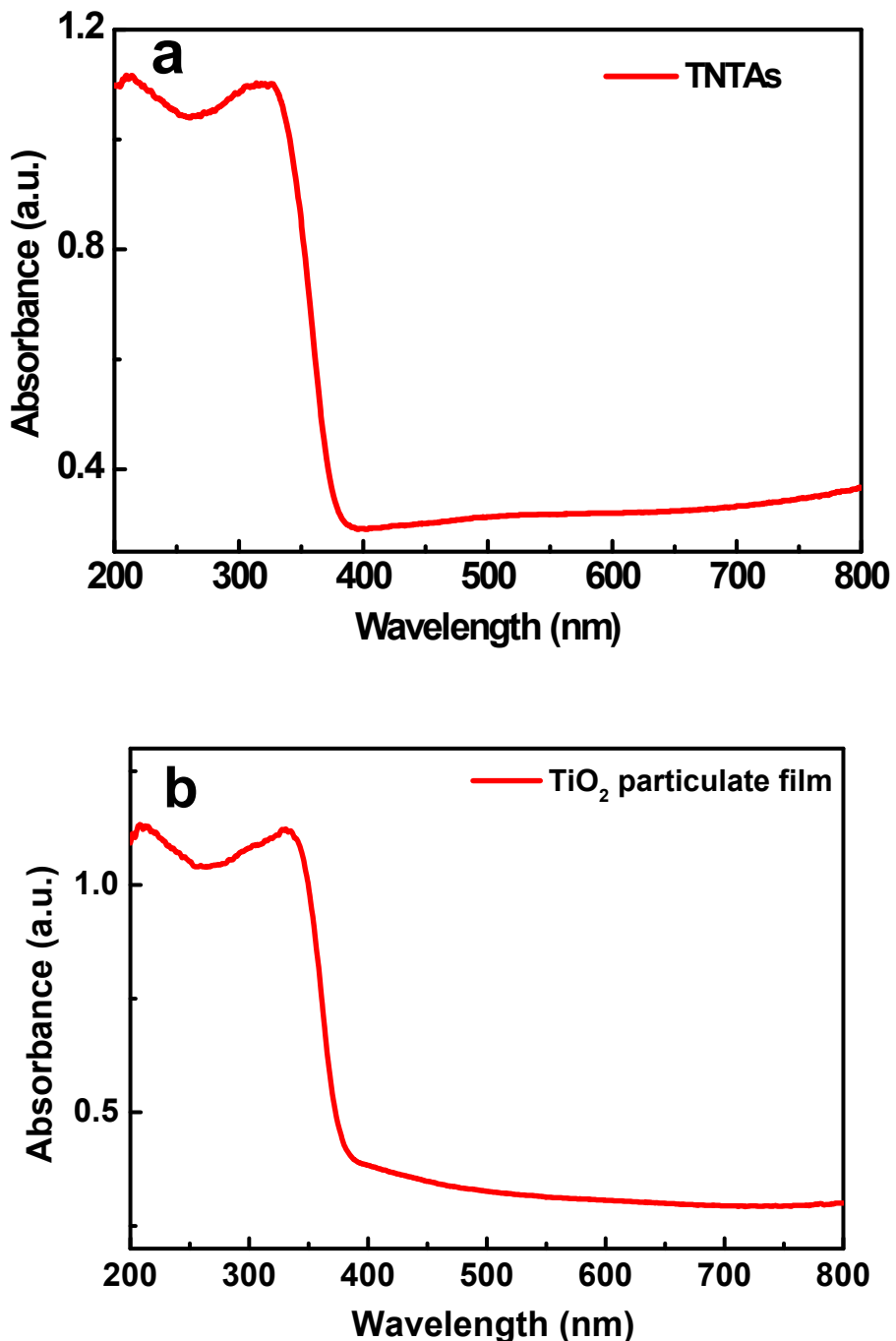


Figure S6. UV-vis diffuse reflectance spectrum (DRS) of (a) NP-TNTAs and (b) TiO_2 particulate

film on Ti foil.

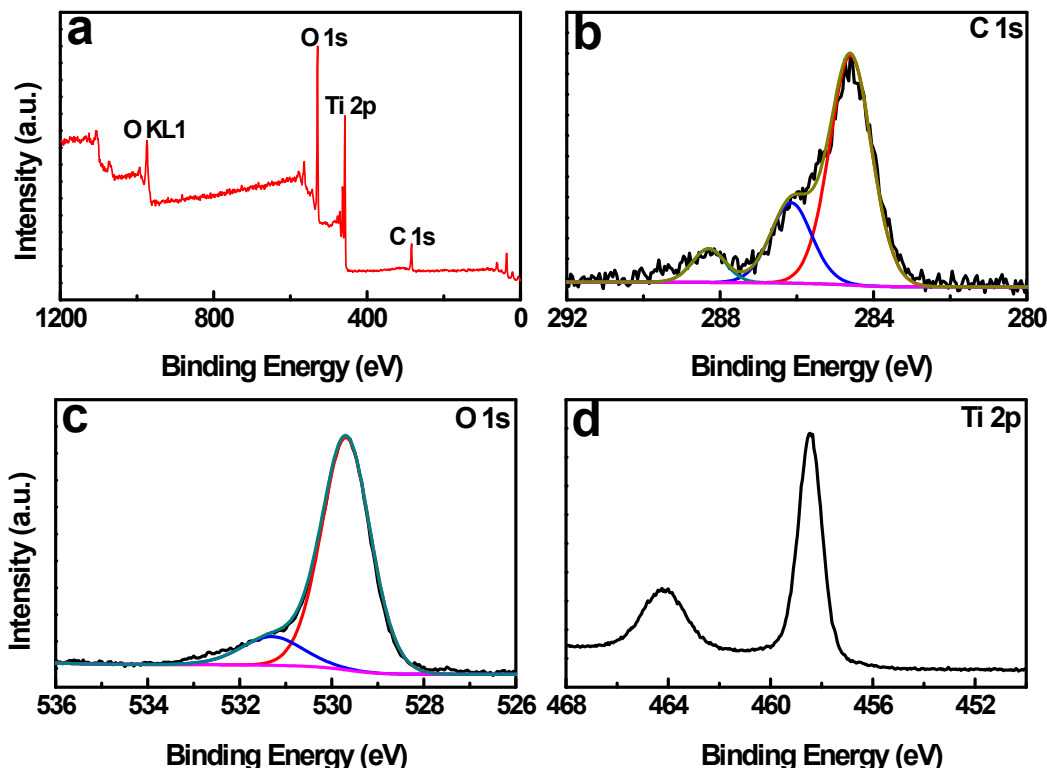


Figure S7. (a) Survey spectrum and high-resolution XPS spectra of (b) C 1s, (c) O 1s, and (d) Ti 2p for blank NP-TNTAs.

Table S1. Chemical species *versus* binding energy for CdSe/NP-TNTAs heterostructure.

<i>Element</i>	<i>CdSe/NP-TNTAs versus NP-TNTAs</i>	<i>Chemical Bond Species</i>
C 1s A	284.59 <i>vs</i> 284.60	C-C/C-H
C 1s B	286.48 <i>vs</i> 286.15	C-OH/C-O-C ¹
C 1s C	288.37 <i>vs</i> 288.30	Carboxylate (CO ₃ ²⁻) ²
O 1s A	529.85 <i>vs</i> 529.69	Lattice Oxygen
O 1s B	530.85 <i>vs</i> 531.30	Ti-OH ³
Ti 2p_{3/2}	458.60 <i>vs</i> 458.45	Anatase (4 ⁺) ⁴
Ti 2p_{1/2}	464.35 <i>vs</i> 464.20	Anatase (4 ⁺)
Cd 3d_{5/2}	404.90	Cd (2 ⁺) ⁵
Cd 3d_{3/2}	411.66	Cd (2 ⁺)
Se 3d_{5/2}	53.45	Se(2-) ^{6,7}

Note: Ti-OH group in CdSe/NP-TNTAs nanocomposite demonstrates substantial blue shift in binding energy as compared with that of blank NP-TNTAs (i.e. 530.85 eV versus 531.30 eV), indicating intimate interfacial interaction between CdSe and NP-TNTAs owing to the formation of heterojunction nanostructure afforded by electrochemical deposition strategy.

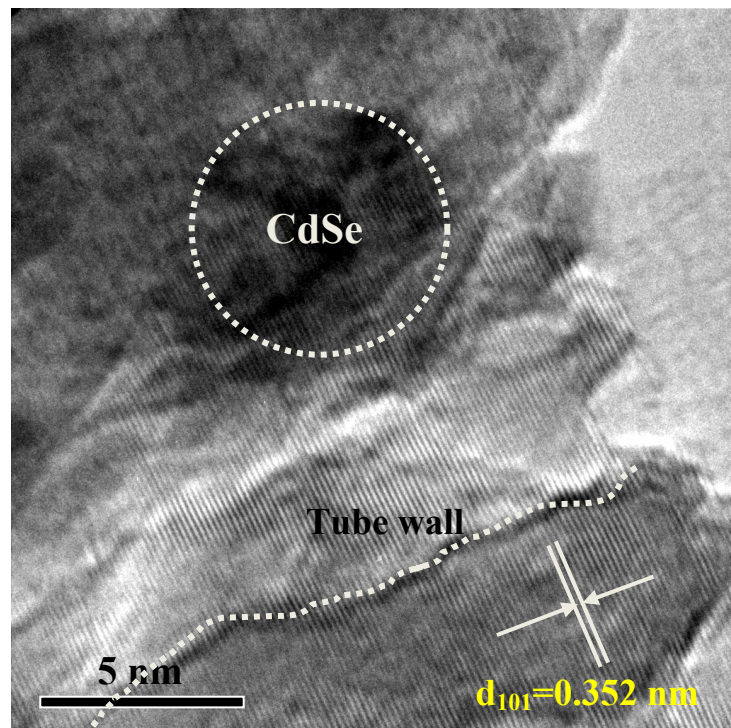


Figure S8. HRTEM image of CdSe deposited on the NP-TNTAs.

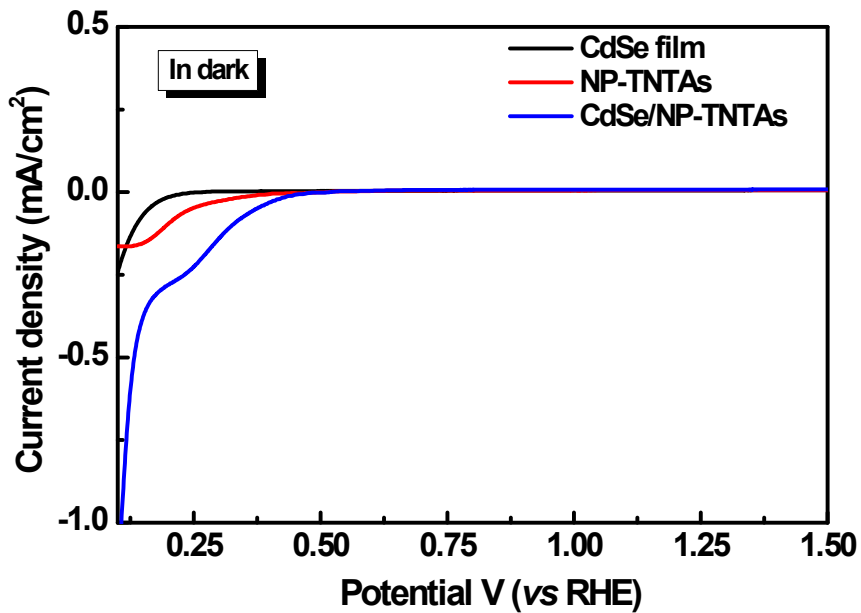


Figure S9. Photocurrent-photovoltage (I-V) curves of blank NP-TNTAs, CdSe film and CdSe/NP-TNTAs heterostructure in dark.

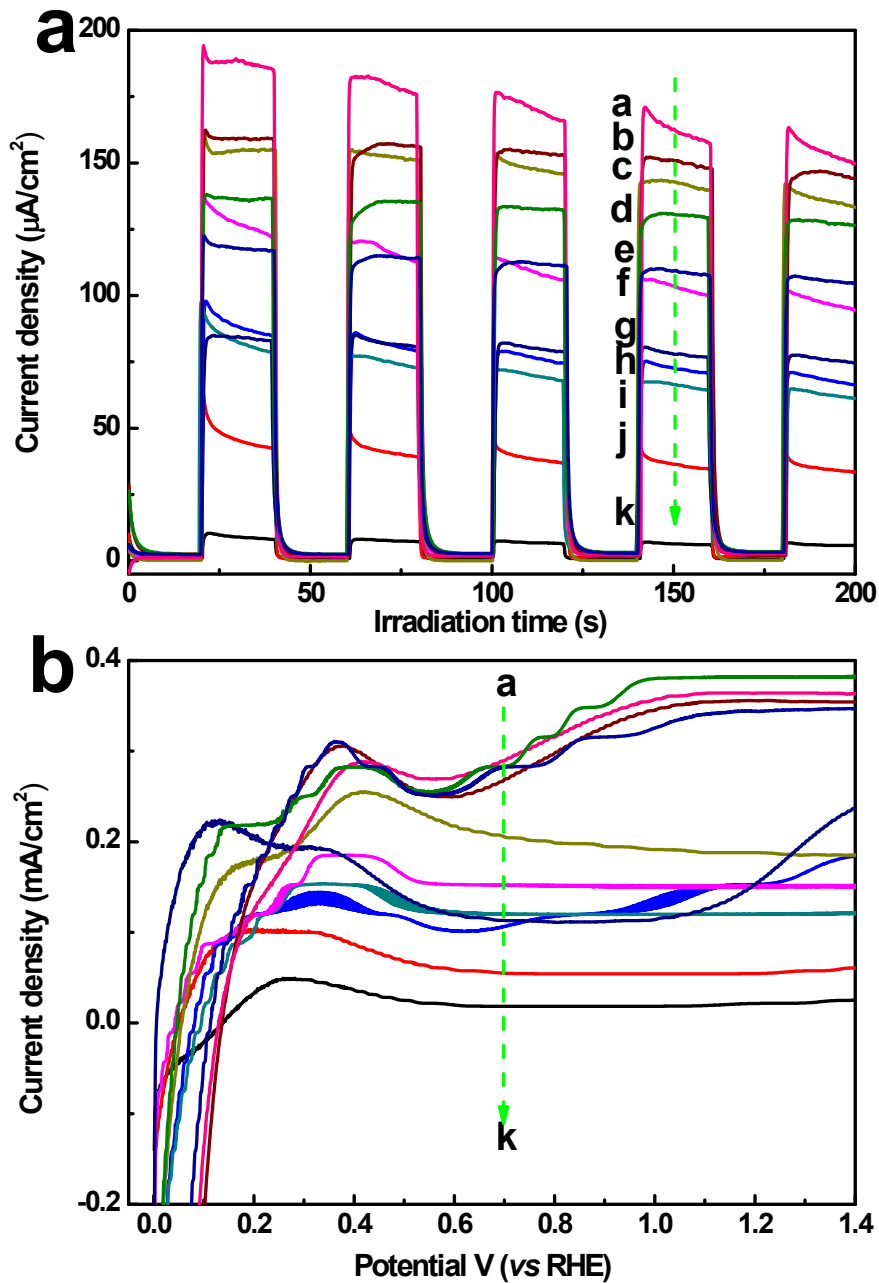


Figure S10. (a) Short-circuit transient photocurrent responses of NP-TNTAs and CdSe/NP-TNTAs heterostructures prepared by different deposition time in 1 M NaOH aqueous solution (pH = 13.9) at open circuit voltage bias *versus* Pt counter electrode under visible light irradiation ($\lambda > 420$ nm), specifically, *a*: 1600 s, *b*: 1400 s, *c*: 1000 s, *d*: 1800 s, *e*: 800 s, *f*: 2000 s, *g*: 1200 s, *h*: 400 s, *i*: 600 s, *j*: 200 s, *k*: blank NP-TNTAs. (b) Photocurrent-photovoltage (I - V) curves of the samples under the same conditions, the scanning rate is 50 mV/s, specifically, *a*: 1600 s, *b*: 1800 s, *c*: 1400 s, *d*: 2000 s, *e*: 1000 s, *f*: 800 s, *g*: 1200 s, *h*: 600 s, *i*: 400 s, *j*: 200 s, *k*: blank NP-TNTAs.

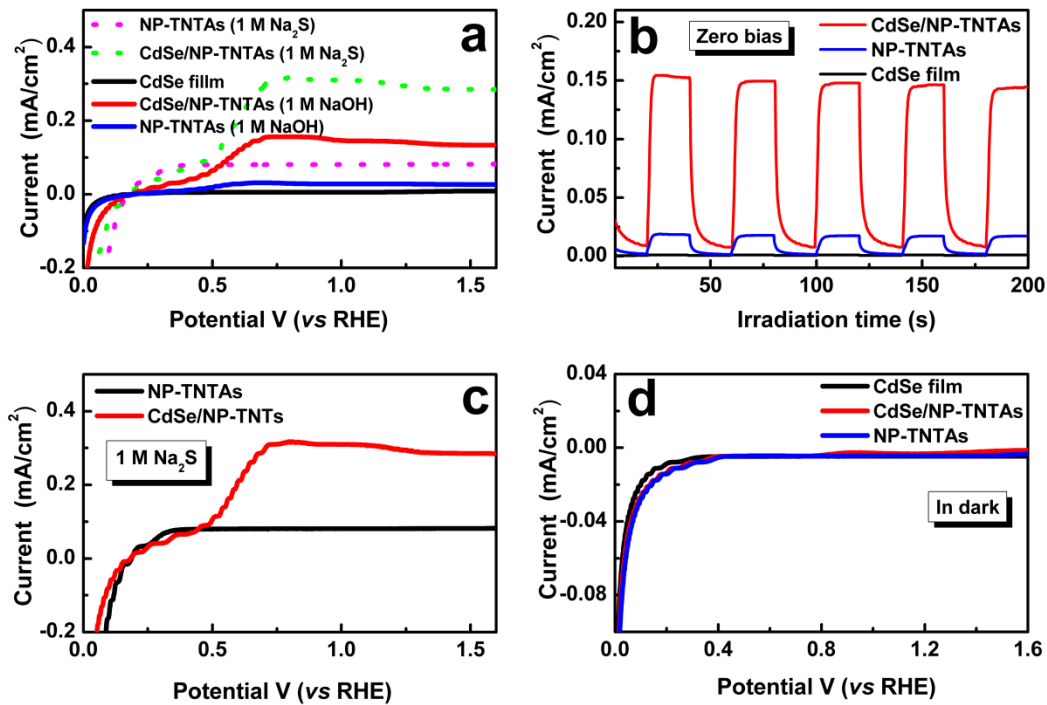


Figure S11. (a) Photocurrent-photovoltage ($J-V$) curves (5 mV/s) of NP-TNTAs, CdSe film and CdSe/NP-TNTAs heterostructure under simulated solar light irradiation (AM 1.5 filter) in 1 M NaOH ($\text{pH} = 13.9$) or 1 M Na_2S aqueous solution, (b) zero-biased short-circuit transient photocurrent responses of NP-TNTAs, CdSe film and CdSe/NP-TNTAs heterostructure under on-off cycles of simulated solar light irradiation (AM 1.5 filter) in 1 M NaOH aqueous solution ($\text{pH} = 13.9$), (c) Photocurrent-photovoltage ($J-V$) curves (5 mV/s) of NP-TNTAs and CdSe/NP-TNTAs heterostructure under simulated solar light irradiation (AM 1.5 filter) in 1 M Na_2S aqueous solution, and (d) Photocurrent-photovoltage ($J-V$) curves (5 mV/s) of the samples in dark.

Note: Photocurrent densities of NP-TNTAs and CdSe/NP-TNTAs heterostructure have been greatly improved when using 1 M Na_2S aqueous solution as the electrolyte, as shown in a and c, indicating the PEC performances of the samples can be tuned by different electrolyte.

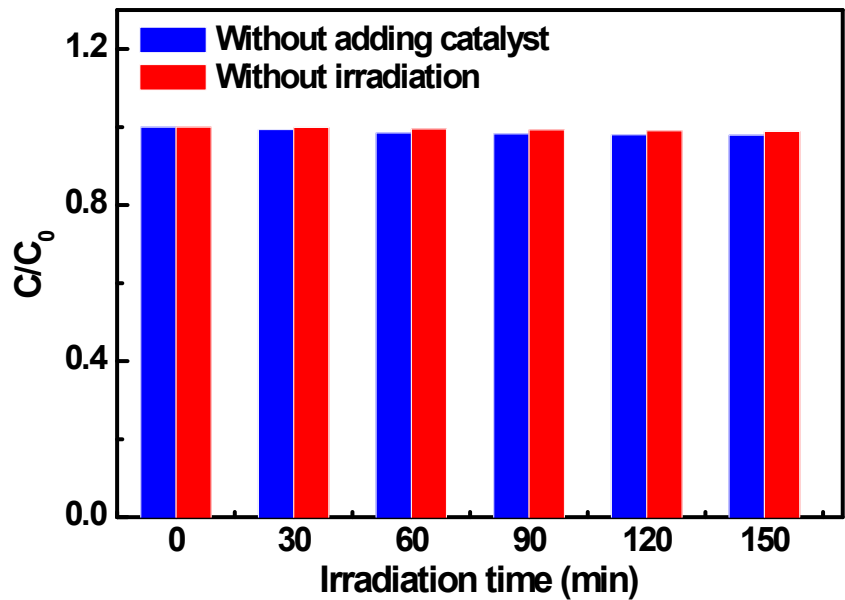


Figure S12. Blank experiments for photodegradation of MO without irradiation or photocatalyst.

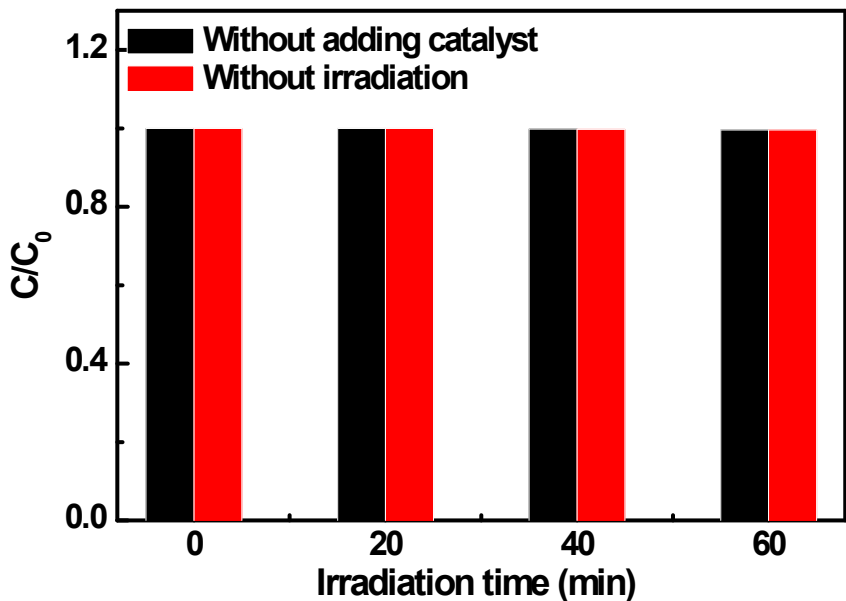


Figure S13. Blank experiments for photocatalytic reduction of 4-NA without irradiation or photocatalyst.

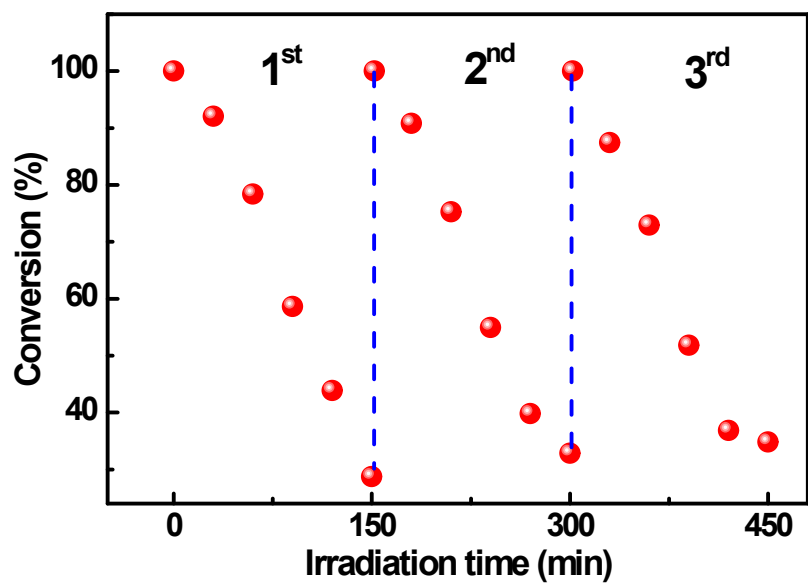


Figure S14. Cycling measurements for photocatalytic reduction of 4-NA over CdSe/NP-TNTAs heterostructure under visible light irradiation ($\lambda > 420$ nm), with the addition of ammonium formate as quencher for photogenerated holes and N₂ purge under ambient conditions.

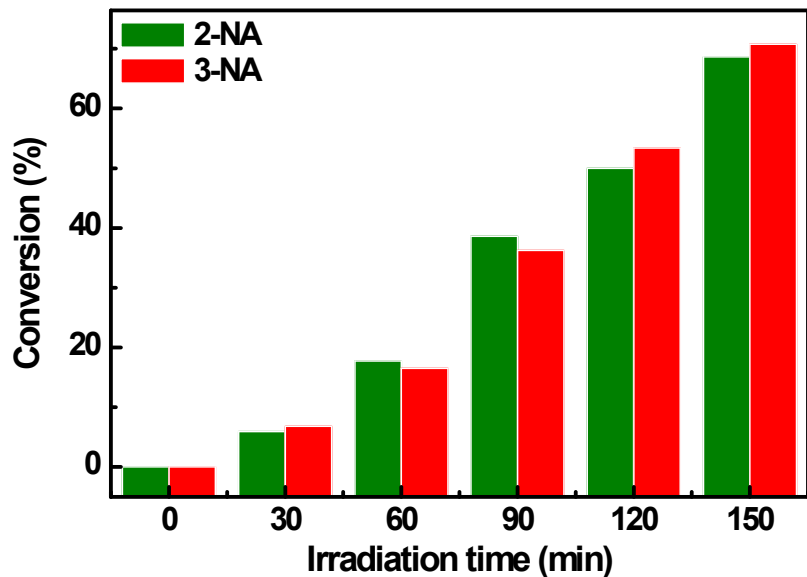


Figure S15. Photocatalytic reduction of 2-NA and 3-NA over different samples under visible light irradiation ($\lambda > 420$ nm), with the addition of ammonium formate as quencher for photogenerated holes and N₂ purge under ambient conditions.

References

- 1 S. Biniak, G. Szymanski, J. Siedlewski and A. Swiatkowski, *Carbon* 1997, **35**, 1799-1810.
- 2 X. M. Wei and H. C. Zeng, *Chem. Mater.* 2003, **15**, 433-442.
- 3 J. Li, S. B. Tang, L. Lu and H. C. Zeng, *J. Am. Chem. Soc.* 2007, **129**, 9401-9409.
- 4 O. I. Micic, M. T. Nenadovic, M. W. Peterson and A. J. Nozik, *J. Phys. Chem.* 1987, **91**, 1295-1297.
- 5 J. Zhang, J. G. Yu, M. Jaroniec and J. R. Gong, *Nano Lett.* 2012, **12**, 4584-4589.
- 6 T. Takahashi, T. Sagawa and H. Hamanaka, *J. Non-Cryst. Solids* 1984, **65**, 261-267.
- 7 L. J. Meng, H. Meng, W. J. Gong, W. Liu and Z. D. Zhang, *Thin Solid Films* 2011, **519**, 7627-7631.